PROCEEDINGS OF SCIENCE

Using Muon Rings for the Optical Throughput Calibration of the Cherenkov Telescope Array

Markus Gaug,[a] **Steven Fegan,**[b] **Alison Mitchell**[*,c] **Maria-Concetta Maccarone,**[d] **Teresa Mineo,**[d] **and Akira Okumura**[e] **for the CTA Consortium**[†]

[a] *Unitat de Física de les Radiacions, Departament de Física, and CERES-IEEC, Universitat Autònoma de Barcelona, E-08193 Bellaterra, Spain*

[b] *Laboratoire Leprince-Ringuet, Ecole Polytéchnique, CNRS/IN2P3, F-91128 Palaiseau, France*

[c] *Physik Institut, Universität Zürich, Winterthurerstrasse 190, CH-8057 Zürich, Switzerland*

[d] *Istituto di Astrofisica Spaziale e Fisica Cosmica di Palermo, INAF, Via Ugo La Malfa 153, I-90146 Palermo, Italy*

[e] *Institute for Space–Earth Environmental Research, and Kobayashi–Maskawa Institute for the Origin of Particles and the Universe, Nagoya University, Furo-cho, Chikusa-ku, Nagoya 464-8602, Japan*

E-mail: markus.gaug@uab.cat, sfegan@llr.in2p3.fr, alison.mitchell@physik.uzh.ch, cettina.maccarone@inaf.it, teresa.mineo@inaf.it, oxon@mac.com

Muon ring images observed with Imaging Atmospheric Cherenkov Telescopes (IACTs) provide a powerful means to calibrate the optical throughput of IACTs and monitor their optical point spread function. We investigate whether muons ring images can be used as the primary optical throughput calibration method for the telescopes of the future Cherenkov Telescope Array (CTA) and find several additional systematic effects in comparison to previous works. To ensure that the method achieves the accuracy required by CTA, these systematic effects need to be taken into account and minor modifications to the hardware and analysis are necessary. We derive analytic estimates for the expected muon data rates to be used for optical throughput calibration, monitoring of the optical point spread function, with achievable statistical and systematic uncertainties, and explore the potential of muon ring images as a secondary method of camera pixel flat-fielding.

36th International Cosmic Ray Conference -ICRC2019-
July 24th - August 1st, 2019
Madison, WI, U.S.A.

[*] Speaker.

[†] for consortium list see PoS(ICRC2019)1177

PoS(ICRC2019)684

1. Introduction

Optical throughput calibration of Imaging Atmospheric Cherenkov Telescopes (IACTs) has been successfully carried out in the past using ring images produced by local muons [1, 2, 3, 4, 5, 6, 7, 8, 9, 10, 11, 12, 13]. Given the clear advantages of the method, such as low cost, good understanding and vast experience, important collateral benefits, CTA has established, as a baseline, optical throughput calibration and monitoring of its Large-, Medium- and Small-Sized-Telescopes (LST, MST and SST), through the thorough analysis of muon rings.

The method has been revisited in a recent paper [14] and its limitations and residual systematic uncertainties assessed. The task is severely complicated by the vast amount of innovative technologies foreseen for the CTA telescopes, like dual-mirror designs [15], telescopes of very different sizes [16], large fields-of-view and hence enormous camera sizes [17], or the use of silicon photomultipliers in certain camera projects [18, 19]. The original method developed by Vacanti et al. [3] needs hence a list of important updates in order to achieve desired accuracies.

2. Requirements for muon calibration

For the muon throughput calibration to achieve the predicted 4% accuracy [14], a series of conditions must be met, which need to be taken into account:

Muon trigger: The telescope cameras must be able to trigger on, and flag prior to transmission of data, fully contained muon rings (see e.g. [20, 21, 22]).

Hard UV blindness: The optical elements of the Cherenkov Telescope must jointly ensure by design that wavelengths below 290 nm in the Cherenkov light spectrum from local muons contribute less than 5% to the observed muon image amplitude. This requirement can actually be monitored with a dedicated illumination device [23].

Chromaticity of degradation: The relative degradation of the system for different wavelengths, i.e. the chromaticity of the degradation, must be assessed externally. Typically, such effects can be monitored on yearly time-scales [23], albeit rather relaxed accuracy requirements of 10–15% are sufficient here.

Unbiased pulse integration and noise removal: The biases introduced by pulse integration and noise removal to the muon analysis must be smaller than 1% of the estimated ring image size.

Correction for non-active pixels: Non-active, broken or unreliable pixels must be correctly taken into accout, and their impact must account for less than 0.5% of the muon image size (see [24]).

Non-spherical reflectors: IACT reflectors are typically not perfectly spherical, but show either an approximately hexagonal structure, or even more complicated polygons. Such structure of the reflector must be taken into account in the muon analysis, e.g. by line integration along the mirror surface as a function of azimuth angle [25].

Plate-scale calibrations: The muon analysis must correct for biases due to optical aberrations in the correspondence of camera coordinates to incidence angles.

Finite camera focus: The muon analysis must correct for finite camera focuses, see Sect. 2.1.

Geomagnetic field effects: The muon analysis must be corrected for geomagnetic field effects, see Sect. 2.2.

Shadow awareness: The muon analysis must include the effect of shadows from the camera and the typical central holes in the reflector, see Sect. 2.3.

Muon simulations: The method must be calibrated, when starting to operate each new telescope, against dedicated muon simulations, which must correctly include all shadowing parts of the telescope, at their respective distances to the reflector. That initial "calibration of the method" is necessary to account for residual shadows (e.g. ropes) not included in the reconstruction.

Extinction of muon Cherenkov light by air molecules and aerosols: The analysis must account for extinction of the muon Cherenkov light by air molecules and aerosols, see Sect. 2.4.

Incidence-angle dependencies: Dependencies of the sensitivity of the camera to light from different incidence angles must be included in the muon analysis, see Sect. 2.3.

Mis-focused mirrors: The muon analysis must be corrected for mis-aligned primary mirrors.

In the following, a small selection of important, but hitherto overlooked, details is presented.

2.1 Finite camera focuses

Large IACTs focus their cameras at the mean altitude at which air shower maxima are observed, normally chosen as 10 km distance above the telescope.

For an ideal telescope of focal length F, focused at infinity, i.e. with the camera placed at $z_f = F$, the Cherenkov angle of the emitted rays equals the radius of the imaged ring. For a telescope focused at a distance x_f, i.e. with the camera placed at z_f with $1/z_f = 1/F - 1/x_f$, the rays from an on-axis muon radiating at distance x will form a ring of radius:

$$\tan\theta_{zf} = \tan\theta_c \cdot (1 - x/x_f) \quad , \tag{2.1}$$

where θ_c denotes the Cherenkov angle. At its highest point, the Cherenkov light from a local muon is imaged into a smaller ring with radius smaller than θ_c, by the time the muon impacts the mirror $(x = 0)$ the angle is the nominal value. This results in a systematic error if the ring radius is directly interpreted as the mean Cherenkov angle. The bias introduced on the reconstructed Cherenkov angle varies from about $\sim -2\%$ to $\sim -4\%$, depending on the muon energy for the MST, whereas for the LST biases can be as high as -8%.

2.2 Geomagnetic field effects

Bending of the muon trajectory in the geomagnetic field has not been considered important so far for local muons. However, it may lead to non-negligible and asymmetric broadening of muon rings, especially for large-sized IACTs located on sites with stronger terrestrial field. A muon of momentum p propagating a distance D perpendicular to the field of strength B will be deflected by an angle $\Delta\theta$:

$$\Delta\theta \quad = \left(\frac{\mathrm{d}\theta}{\mathrm{d}x}\right)\cdot x \quad = 6.9\times10^{-5}\ (\mathrm{deg/m})\cdot\left(\frac{10\ \mathrm{GeV}}{p}\right)\cdot\left(\frac{B_\perp}{40\ \mu\mathrm{T}}\right)\cdot\left(\frac{x}{\mathrm{m}}\right) \tag{2.2}$$

where $B_\perp$ the magnetic field component perpendicular to the muon's velocity. Its maximum value can be assumed as $B \approx 40\ \mu$T, achieved at La Palma at a zenith angle of $\sim 40^\circ$.

The bias for the reconstructed Cherenkov angle can reach up to 2% in the worst case of a full muon ring imaged into an LST camera, under the maximum impact distance and the azimuthal component of the $B_\perp$ parallel to the azimuth component of the impact parameter.

2.3 Non-negligible inclination angles and camera shadows

Muon inclination angles υ were so far limited to $\upsilon \lesssim 1^\circ$ for field-of-view cameras $\lesssim 5^\circ$, with associated effects on the throughput calibration of only $\lesssim 0.05\%$. However, wide-field cameras for CTA with up to 10° field-of-view can regularly obtain muon images with ring centers up to 3.5° from the camera center, resulting in an effect on the modulated signal along the ring of $\lesssim 0.3\%$.

The situation becomes more complicated when central shadowing objects, such as the camera, are considered. For telescopes with a focal ratio of f, the shadow produced by the camera moves with inclination angle approximately as $\Delta \approx f\cdot\upsilon$, slightly exceeding the intrinsic resolution, with which the muon impact distance can be obtained.

Furthermore, the square shape of some camera designs (like the MST and the LST) introduces dependencies of the reconstructed optical throughput on the muon inclination angle, see Fig. 1. The effect of such a quadratic shape can nevertheless be included in the analytical model, as well as the additional shadow of the central hole.

2.4 Extinction of muon Cherenkov light

A photon of energy ε emitted at a distance x from the telescope suffers molecular and aerosol extinction. One can describe the atmospheric transmission for the photon as:

$$T(\varepsilon,x;\vartheta) = \exp\Big(-\int_0^{x\cdot\cos\vartheta}\left[\alpha_{\mathrm{mol}}(\varepsilon,h)+\alpha_{\mathrm{aer}}(\varepsilon,h)\right]\,\mathrm{d}h/\cos\vartheta\Big) \quad , \tag{2.3}$$

where α_{mol} and α_{aer} are the volume extinction coefficients from molecular and aerosol extinction at an altitude h, respectively, and the telescope itself points to the sky under a zenith angle ϑ.

Large telescopes are more prone to variations of the atmospheric extinction because they observe local muons emitting from higher altitudes. We simulated typical variations of the molecular profile at La Palma [26] and found peak-to-peak variations of the molecular transmission smaller than 0.2%. Nevertheless, aerosol transmission can be affected by dust intrusions, particularly at La Palma. In the case of strong aerosol densities, very close to the ground, a correction of $\lesssim 3\%$ needs to be applied. This problem can be either circumvented by adequate data selection, or by applying a bias correction, which can be calculated once the aerosol profile is assessed.

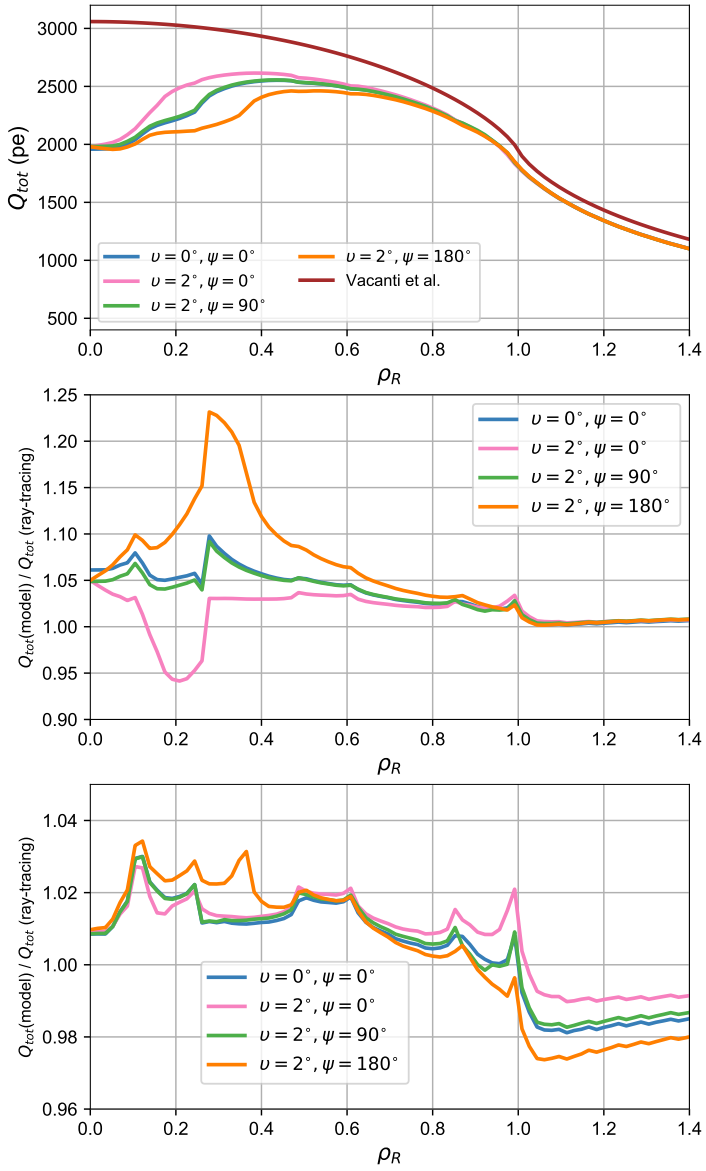

Figure 1: Expected effect of shadowing of the MST's square camera on the total amount of photons collected (top). In full brown, Vacanti's solution [3] is plotted without considering the shadow. The full blue lines show the true value for an on-axis muon, and the orange, green and pink lines show instead the case for a 2° inclined muon, with azimuthal incidence angles of 0°, 90°, and 180°. The center plot shows the relative values of the latter cases, compared to the analytical roundish camera model and the bottom plot with the analytical square camera model and the improved shadow models. Note the different y-axis scales of the center and bottom plots. With the full shadow model, a peak-to-peak difference in modelled and simulated photon yield between the investigated impact distances and muon inclination angles of only about 4% is observed, if fully contained rings are considered.

3. Additional use of muon calibration

Contrary to the Cherenkov light from gamma-ray induced showers, Cherenkov light from local muons does not illuminate the reflector uniformly, but is instead concentrated at the muon impact point. Moreover, the expected fluence of Cherenkov light at each camera pixel can be predicted to good accuracy [14]. For these reasons, muon calibration delivers additional calibration information, which can be exploited for alternative calibrations and used for monitoring:

Pixel-wise charge calibration: Flat-fielding coefficients from muon analysis can be used to monitor and improve the accuracy of the coefficients obtained through the typical camera flat-fielding.

Pixel-wise time calibration: Time offset coefficients from muon analysis can be used to monitor and improve the accuracy of the coefficients obtained with the flat-fielding procedure.

Optical PSF monitoring: Estimates of the optical point spread function (PSF) of each telescope from muon analysis can be used to monitor and improve its accuracy.

Degradation of individual mirrors: Estimates of the relative reflectance of each mirror with respect to the telescope average can be obtained from muon analysis.

Table 1 lists the expected achievable rates, with which each monitoring point can be obtained to a precision comparable with the expected accuracy of the same monitoring point (see [14] for details). One can see that the needed monitoring times are typically shorter than the duration of one science observation run.

	LST		MST		SST	
	$\vartheta = 0°$	$\vartheta = 60°$	$\vartheta = 0°$	$\vartheta = 60°$	$\vartheta = 0°$	$\vartheta = 60°$
	Determination of optical throughput					
Rate (Hz)	1.8	0.5	5	1.4	0.8	0.2
Monitoring time	14 s	48 s	5 s	18 s	28 min	18 min
	Determination of optical throughput (per pixel)					
Rate (Hz)	0.07	0.02	0.10	0.03	0.02	0.006
Monitoring time	6 min	21 min	4 min	13 min	2.3 h	7.6 h
	Determination of time offset (per pixel)					
Rate (Hz)	0.1	0.03	0.2	0.04	0.03	0.008
Monitoring time	10 s	36 s	6 s	23 s	36 s	2.2 min
	Determination of optical PSF					
Rate (Hz)	5	1.6	8	2.5	2.4	0.7
Monitoring time	9 s	25 s	5 s	16 s	17 s	1 min

Table 1: Expected rates of high quality, fully contained muon ring images for calibration for the proposed telescopes of CTA, and the corresponding monitoring time scales.

4. Conclusions

Using algorithms from Vacanti et al. [3], several authors have claimed a theoretical accuracy of as good as ∼2% for the optical throughput calibration of IACTs using images from local muons. To ensure that the method achieves the accuracy required by CTA, we revisited all documented algorithms and systematic effects [14] and found several effects, which have not been taken into account so far, or which appear non-negligible for large mirrors, or large square-shaped cameras, or the dual-mirror telescope designs proposed for CTA.

Most of these effects can be corrected by a careful analysis. Nevertheless, a few systematic effects will require dedicated studies or even adaptation in the design of the hardware employed for the CTA telescopes to achieve the desired accuracy. These effects are mostly related to the differences in the observed spectrum of Cherenkov light between local muons and distant gamma-ray showers.

We find that after incorporating all effects, the optical throughput of the full telescope can be determined with an accuracy of better than 4% (LST and MST) and 5% (SST).

Muon calibration allows one to monitor additionally, and without much effort the flat-fielding of the camera, and to provide the relative time offsets of each pixel. Similarly, differences in reflectance among the mirrors can be detected by plotting the retrieved optical bandwidth as a function of reconstructed impact point.

Finally, contrary to the starlight, the light from local muons gets registered within sub-nanosecond time windows, which allows one to greatly reduce residual backgrounds from the night sky and unresolved stars and monitor the optical point spread function of each telescope.

References

[1] P. Fleury et al., *Čerenkov ring images of cosmic ray muons*. Proc. 22nd ICRC, Dublin **2** 595, 1991.

[2] Jiang, Y., Fleury, P., Lewis, A. D., et al. *Absolute Calibration of an Atmospheric Cherenkov Telescope Using Muon Ring Images*. Proc. 23rd ICRC **4** 662, 1993.

[3] Vacanti, G., Fleury, P., Jiang, Y., et al. *Muon ring images with an atmospheric Čerenkov telescope Astrop. Phys.* **2**, 1–11, 1994.

[4] Rose, H. J. *Cherenkov Telescope Calibration using Muon Ring Images*. Proc. 24th ICRC **3** 464, 1995.

[5] Rovero, A. C., Buckley, J. H., Fleury, P., et al. *Calibration of the Whipple atmospheric Čherenkov telescope Astrop. Phys.* **5**, 27–34, 1996.

[6] Pühlhofer, G., Bolz, O., Götting, N., et al. *The technical performance of the HEGRA system of imaging air Cherenkov telescopes Astrop. Phys.* **20**, 267–291, 2003.

[7] Leroy, N., Bolz, O., Guy, J., et al. *Calibration Results for the First Two H.E.S.S. Array Telescopes* Proc. 28th ICRC **5** 2895, 2003.

[8] Shayduk, M., Kalekin, O., Mase, K., Pavel, N., MAGIC Collaboration *Calibration of the MAGIC Telescope Using Muon Ring Images*, Proc. 28th ICRC, Tsukuba **5** 2951, 2003.

[9] Meyer, M., et al. *Analysis of muon events recorded with the MAGIC telescope*. High Energy Gamma-Ray Astronomy **745** 774–778, 2005.

[10] Goebel, F., Mase, K., Meyer, M., et al. *Absolute energy scale calibration of the MAGIC telescope using muon images*. Proc. 29th ICRC **5** 179, 2005.

[11] Humensky, T. B. *Calibration of VERITAS Telescope 1 via Muons*. Proc. 29th ICRC, Pune, 2005 [ArXiv:astro-ph/0507449]

[12] Hanna, D. *Calibration Techniques for VERITAS*. Proc. 30th ICRC, Merida **3** 1417–1420, 2008.

[13] Chalme-Calvet, R., de Naurois, M., Tavernet, J.-P. for the H. E. S. S. Collaboration *Muon efficiency of the H.E.S.S. telescope*. Proc. AtmoHEAD Conf., Saclay 2014. [arXiv:1403.4550]

[14] M. Gaug, S. Fegan, A. M. W. Mitchell, M. C. Maccarone, T. Mineo, A. Okumura, *Using Muon Rings for the Calibration of the Cherenkov Telescope Array: A Systematic Review of the Method and Its Potential Accuracy*, *Astrophys. J. Suppl.* **243** 11, 2019 [arXiv:1907.04375].

[15] V. Vassiliev, S. Fegan and P. Brousseau, *Wide field aplanatic two-mirror telescopes for ground-based γ-ray astronomy*, *Astroparticle Physics* **28** 10-27, 2007.

[16] The CTA Consortium: Actis, M. et al., *Design concepts for the Cherenkov Telescope Array CTA: an advanced facility for ground-based high-energy gamma-ray astronomy*, *Experimental Astronomy* **32** 193-316, 2011 [arXiv:1008.3703]

[17] T. Tavernier et al., *Status and performance results from NectarCam, a camera for CTA MST's*, these proceedings.

[18] Billotta, S. et al. *SiPM Detectors for the ASTRI project in the framework of the Cherenkov Telescope Array*, *Proc. SPIE Astronomical Telescopes + Instrumentation* **9154** 91541R, 2014.

[19] C. Alispach et al., *Calibration strategy for the next generation of SiPM cameras*, these proceedings.

[20] M. C. Maccarone et al., *Pre-selecting muon events in the camera server of the ASTRI telescopes for the Cherenkov Telescope Array*, *Proc. SPIE* **9913** 991370, 2016.

[21] T. Mineo et al., *Muon calibration of the ASTRI-Horn telescope: preliminary results*, these proceedings.

[22] R. Pillera et al., *Muon tagging on the BEE of CHEC-S – a compact high-energy camera for CTA*, these proceedings.

[23] A. Segreto et al., *The absolute calibration strategy of the ASTRI SST-2M telescope proposed for the Cherenkov Telescope Array and its external ground-based illumination system*, *Proc. SPIE Ground-based and Airborne Telescopes VI* **9906** 99063S, 2016.

[24] A. Mitchell, *Optical Efficiency Calibration for Inhomogeneous IACT Arrays and a Detailed Study of the Highly Extended Pulsar Wind Nebula HESS J1825-137*, PhD thesis, University Heidelberg, 2016.

[25] A. Mitchell, V. Marandon, and D. Parsons *A Generic Algorithm for IACT Optical Efficiency Calibration using Muons Proc. 34th ICRC, The Hague* **236** 1, 2016 [arXiv:1509.042587]

[26] P. Munar-Adrover and M. Gaug, *Studying molecular profiles above the Cherenkov Telescope Array sites*, *EPJ* **197** 01002, 2019.

Acknowledgments

This work was conducted in the context of the CTA Central Calibration Facilities Working Group. We gratefully acknowledge financial support from the agencies and organizations listed here: http://www.cta-observatory.org/consortium_acknowledgments
This proceeding has gone through internal review by the CTA Consortium.